Microstructure of Cesium Hydrogen Salts of 12-Tungstophosphoric Acid Relevant to Novel Acid Catalysis†

Toshio Okuhara,*,‡ Hiromu Watanabe,§ Toru Nishimura,|| Kei Inumaru,⊥ and Makoto Misono*,#

Department of Applied Chemistry, Graduate School of Engineering, The University of Tokyo, Bunkyo-ku, Tokyo 113-8656, Japan

Received December 6, 1999. Revised Manuscript Received May 4, 2000

A comprehensive interpretation of the microstructure and mechanism of the formation of a versatile solid acid catalyst, $Cs_{2.5}H_{0.5}PW_{12}O_{40}$, has been attempted by combining the new results obtained with solid-state NMR, XRD, SEM, and N_2 porosimetry with the data reported previously. The precipitates of $Cs_{2.5}H_{0.5}PW_{12}O_{40}$ just formed from aqueous solutions of $H_3PW_{12}O_{40}$ and Cs_2CO_3 consist of ultrafine crystallites in which the acid form, $H_3PW_{12}O_{40}$, is epitaxially deposited on the surface of $Cs_3PW_{12}O_{40}$ crystallites. Calcination of the precipitates brings about the migration of H^+ and Cs^+ in the solid to form a nearly uniform solid solution in which protons distribute randomly through the entire bulk, as revealed by XRD and ^{31}P solid-state NMR. Impregnation of $Cs_3PW_{12}O_{40}$ with the aqueous solution of $H_3PW_{12}O_{40}$ also gives the uniform salt after calcination. Pore-size distribution evaluated by the analysis of N_2 desorption isotherm showed that $Cs_{2.5}H_{0.5}PW_{12}O_{40}$ has mesopores as well as micropores that are interparticle voids of the crystallites. The initial heat of NH_3 sorption indicated the presence of very strong acid sites on $Cs_{2.5}H_{0.5}PW_{12}O_{40}$. High catalytic activity of $Cs_{2.5}H_{0.5}PW_{12}O_{40}$ reported for solid−liquid reaction systems is thus principally attributed to the strength and number of acid sites and the mesoporous structure appropriate for the rapid diffusion of molecules.

Introduction

Heteropolyacids and their acidic salts having the Keggin structure are known to be excellent acid catalysts.[1−8] The Keggin structure is composed of a central tetrahedron (XO_4, X = P, Si, Ge, etc.) surrounded by 12 MO_6 octahedra (M = W, Mo, or V) arranged in four groups of three-edge-sharing M_3O_{13}.[9] Heteropolyacids are now utilized as solid acids in several industrial chemical processes such as hydrations of *n*-butene and isobutylene, polymerization of tetrahydrofuran, synthesis of acetic acid from ethylene, etc.[1,2,10,11]

One of the characteristics of a heteropoly compound as a solid acid is the strong acidity. Jozefowicz et al.[12a] and Lafevre et al.[12b] reported the initial heat of NH_3 sorption was about 200 kJ mol^{-1} for $H_3PW_{12}O_{40}$, which was much higher than those of H-ZSM-5 and SiO_2−Al_2O_3. They inferred that $H_3PW_{12}O_{40}$ can be classified as a superacid.[12] The Hammett indicator test also suggested that $H_3PW_{12}O_{40}$ possesses superacidity.[13] Thermal desorption of probe base molecules such as ammonia and pyridine revealed that solid $H_3PW_{12}O_{40}$ is a stronger acid than SiO_2−Al_2O_3 and H-ZSM-5.[14] More recently, Drago et al.[15a] determined the following order of acid strength by calorimetric titration: H_3-

† Catalysis by Heteropoly Compounds 43. See Part 42: Koyano, G.; Ueno, K.; Misono, M. *Appl. Catal.* **1999**, *181*, 267.

* To whom correspondence should be addressed.

‡ Present address: Graduate School of Environmental Earth Science, Hokkaido University, Sapporo 060-0810, Japan. Fax: 81-11-706-4513. E-mail: oku@ees.hokudai.ac.jp.

§ Present address: Mitsubishi Chemical Co. Ltd., 3-1, Chuo-Hacchome, Amicho, Inashiki-gun, Ibaraki 300-0332, Japan.

|| Present address: Mitsui Chemicals, Inc., 580-32, Sodegaura, Sodegaura-shi, Chiba 299-0265, Japan. Japan.

⊥ Present address: Faculty of Engineering, Hiroshima University, Higashi-hiroshima, Hiroshima 739-8527, Japan.

Present address: Department of Environmental Chemical Engineering, Kogakuin University, 1-24-2 Nishi-shinjuku, Shinjuku-ku, Tokyo 163-8677, Japan. Fax: 81-3-3340-0147. E-mail: misono@cc.kogakuin.ac.jp.

(1) Misono, M. *Catal. Rev.-Sci. Eng.* **1987**, *29*, 269; **1988**, *30*, 339.
(2) Okuhara, T.; Mizuno, N.; Misono, M. *Adv. Catal.* **1996**, *41*, 113.
(3) Pope, M. T.; Muller, A. *Angew. Chem., Int. Ed. Engl.* **1991**, *30*, 34.
(4) Izumi, Y.; Urabe, K.; Onaka, M. *Zeolite, Clay, and Heteropoly Acid in Organic Reactions*; Kodansha: Tokyo and VCH: Weinheim, New York, 1992.
(5) Kozhevnikov, I. V. *Catal. Rev.-Sci. Eng.* **1995**, *37*, 311.
(6) Hill, C. L.; Prosse-McCartha, C. M. *Coord. Chem. Rev.* **1995**, *143*, 407.
(7) Corma, A. *Chem. Rev.* **1995**, *95*, 559.
(8) Mizuno, N.; Misono, M. *Chem. Rev.* **1998**, *98*, 199.
(9) Pope, M. T. *Heteropoly and Isopoly Oxometalates*; Springer-Verlag: New York, 1983; Tsigdinos, G. A. *Top. Curr. Chem.* **1978**, *76*, 1.
(10) Misono, M.; Nojiri, N. *Appl. Catal.* **1990**, *64*, 1.
(11) Suzuki, T.; Yoshikawa, Y.; Abe, K. Japanese Patent, Tokkaihei 7-89896, 1995.
(12) (a) Jozefowicz, L. C.; Karge, H. G.; Vasilyeva, E.; Moffat. J. B. *Microporous Mater. 1*, 313. (b) Lefevre, F.; Liu-Cai, F. X.; Auroux, A. *J. Mater. Chem.* **1994**, *4*, 125.
(13) Okuhara, T.; Nishimura, T.; Watanabe, H.; Misono, M. *J. Mol. Catal.* **1992**, *74*, 247.
(14) Misono, M.; Mizuno, N.; Katamura, K.; Kasai, A.; Konishi, Y.; Sakata, K.; Okuhara, T.; Yoneda, Y. *Bull. Chem. Soc. Jpn.* **1982**, *55*, 400.
(15) (a) Drago, R. S.; Dias, J. A.; Maier, T. *J. Am. Chem. Soc.* **1997**, *119*, 7702. (b) Essayem, N.; Coudurier, G.; Vedrine, J. C.; Habermacher, D.; Sommer, J. *J. Catal.* **1999**, *183*, 292.

10.1021/cm9907561 CCC: $19.00
Published on Web 07/14/2000

$PW_{12}O_{40} > CF_3SO_3H > p\text{-}CH_3C_6H_4SO_3H \sim H_2SO_4 > CF_3COOH > ClC_6H_4COOH$. On the other hand, Essayem et al.[15b] claimed from the results of exchange between isobutane and $D_3PW_{12}O_{40}$ that $H_3PW_{12}O_{40}$ is not a superacid.

Although the acid form itself is a useful solid acid, the amount of acid sites on the surface is small because of the low surface area (about 5 $m^2\ g^{-1}$). Increasing the number of surface acid sites is indispensable for the development of prominent solid acids (except for the case of pseudo-liquid-phase catalysis[1,2]). The substitution for H^+ by alkaline cations exhibits interesting effects on the surface area and pore structure.[16−18] The salts with large monovalent ions such as Cs^+ are insoluble and possess high surface areas.[16−18] We have demonstrated that partial substitution for H^+ of the heteropolyacid by Cs^+ brings about unique changes in the surface area and hence the acid amount on the surface;[19] the amount of acid site on the surface (called surface acidity) showed a maximum at $x = 2.5$ in $Cs_xH_{3-x}PW_{12}O_{40}$.[17a] Furthermore, $Cs_{2.5}H_{0.5}PW_{12}O_{40}$ was found to be much more active than the parent acid form and other known solid acid catalysts for direct decomposition of ester,[20] alkylation of aromatics,[13,21] acylation,[22] alkylation of isobutane,[23−25] skeletal isomerization of *n*-butane,[26,27] hydrolysis of esters in excess water,[28] and hydration of olefins in a solid−water reaction system.[29] Guyaud et al.[24b] recently reported that the acidic Cs salts prepared by grinding $H_3PW_{12}O_{40}$ with $Cs_3PW_{12}O_{40}$ were highly active for *n*-butane isomerization. It was preliminarily reported by us with solid-state ^{31}P NMR that protons of Cs2.5 distribute nearly statistically through the whole bulk.[13,30] In addition, to explain the changes in the surface area, the surface acidity, and the catalytic activity with the Cs content, the preparation processes of Cs*x* have been tentatively proposed in our previous paper.[26b]

The present study has attempted to provide a comprehensive understanding of the preparation processes, the microstructure, the pore structure, and the surface chemical properties to provide basic knowledge to explain the above-mentioned unique catalysis of the acidic Cs salt of $H_3PW_{12}O_{40}$. The microstructure of the particles, the state of the agglomeration, the pore structure, the proton distribution, and the acidic property have been investigated in a systematic way by using XRD, SEM, solid-state NMR, porosimetry by N_2, and calorimetry of NH_3 sorption. The novel catalysis of $Cs_{2.5}H_{0.5}PW_{12}O_{40}$ has been discussed in relation to these chemical and physical properties.

Experimental Section

Catalysts. $H_3PW_{12}O_{40}\cdot nH_2O$ (Nippon Inorganic Color and Chemical Co. Ltd.) was purified by extraction with diethyl ether and recrystallization from water at room temperature. By evacuation of the crystallites at 323 K for 5 h, $H_3PW_{12}O_{40}\cdot 6H_2O$ was obtained. $H_3PW_{12}O_{40}\cdot 6H_2O$ and Cs_2CO_3 (Merck, extra pure, evacuated at 723 K) were used for the preparation of each aqueous solution. During the procedure, the solid samples were carefully handled in a dry bag to avoid exposure to air and moisture.

Acidic cesium salts, $Cs_xH_{3-x}PW_{12}O_{40}$, were prepared by a titration method or an impregnation method.[13,17,19] In the former, an appropriate amount of the aqueous solution of Cs_2CO_3 (0.10 mol·dm^{-3}) was added dropwise with a constant rate of about 1 $cm^3\cdot min^{-1}$ to the aqueous solution of $H_3PW_{12}O_{40}$ (0.08 mol·dm^{-3}, 20 cm^3) at room temperature with vigorous stirring. The Cs content, *x* in $Cs_xH_{3-x}PW_{12}O_{40}$, was adjusted by the amount of Cs_2CO_3 solution added. From the beginning of the addition of Cs_2CO_3, very fine particle (precipitates) were formed to make the solution milky. After the solution was aged at room temperature overnight, the water was slowly removed by evaporation at 323 K. The resulting solid was ground into white powder. These salts are denoted as Cs*x*. In the latter, the predetermined amount of $Cs_3PW_{12}O_{40}$ prepared by the titration method was impregnated with the aqueous $H_3PW_{12}O_{40}$ solution (0.08 mol·dm^{-3}, 20 cm^3) so as to make the $Cs/PW_{12}O_{40}$ ratio *x*. After aging at room-temperature overnight, the suspension was evaporated to dryness at 323 K in air as in the case of Cs*x*. These salts are denoted as Cs*x*(Imp). The water contents of these solids were determined by a microbalance (Seiko Instruments, SSC5200).[26a]

Characterization by NMR and XRD. Solid-state ^{31}P NMR spectra of $Cs_xH_{3-x}PW_{12}O_{40}$ were obtained with magic-angle spinning (MAS) on a Fourier transform pulsed NMR spectrometer (JEOL JNM-GX270) at room temperature.[31] The sample was evacuated at an elevated temperature for 2 h and then was transferred to a rotor equipped with a Viton O-ring cap in a glovebox. Because the NMR spectra of $Cs_xH_{3-x}PW_{12}O_{40}$ were very sensitive to the moisture, the sample was carefully treated in a dry bag. The spectra were taken at 109.2 MHz with a high-power proton decoupling. The chemical shifts were referenced to 15 mol·dm^{-3} of H_3PO_4 as an external standard.[31]

The powder X-ray diffraction patterns of $Cs_xH_{3-x}PW_{12}O_{40}$ were recorded on an X-ray diffractometer (MAC Science, MXP^3) with CuKα radiation (30 kV− 40 mA). The sample was pretreated at 298 K or an elevated temperature in a vacuum, and XRD spectra were taken in a flow of N_2 to avoid the adsorption of water. The scanning was done from $2\theta = 65°$ to $2\theta = 5°$ at a rate of 0.5° min^{-1}. Si powder (Nacalai Tesque) was used as an internal standard (33 wt %).

Other Measurements. The concentrations of Cs and W in the supernatant and precipitate in the suspension were determined by ICP after the aging for both the titration and impregnation methods, after the suspension was separated by

(16) Niiyama, H.; Saito, Y.; Echigoya, E. *Proceedings of the 7th International Congress on Catalysis, 1980*; Kodansha: Tokyo, Elsevier: Amsterdam, 1981; p 1416.
(17) (a) Okuhara, T.; Nishimura, T.; Misono, M. *Proceedings of the 11th International Congress on Catalysis*; Hightower, J. W., Delgass, W. N., Iglesia, E., Bell, A. T., Eds.; Elseiver: Amsterdam, 1996; pp 581. (b) Okuhara, T.; Kasai, A.; Hayakawa, N.; Yoneda, Y.; Misono, M. *J. Catal.* **1983**, *121*, 83.
(18) Moffat, J. B. *J. Mol. Catal.* **1989**, *52*, 169.
(19) Tatematsu, S.; Hibi, T.; Okuhara, T.; Misono, M. *Chem. Lett.* **1984**, 865.
(20) Okuhara, T.; Nishimura, T.; Ohashi, K.; Misono, M. *Chem. Lett.* **1990**, 1201.
(21) Nishimura, T.; Okuhara, T.; Misono, M. *Appl. Catal.* **1991**, *73*, L7.
(22) Izumi, Y.; Ogawa, M.; Nohara, W.; Urabe, K. *Chem. Lett.* **1992**, 1987.
(23) Okuhara, T.; Yamashita, M.; Na, K.; Misono, M. *Chem. Lett.* **1994**, 1451.
(24) (a) Essayem, N.; Kieger, S.; Coudurier, G.; Vedrine, J. C. *Proceedings of the 11th International Congress on Catalysis*; Hightower, J. W., Delgass, W. N., Iglesia, E., Bell, A. T., Eds.; Elsevier: Amsterdam, 1996; pp 591. (b) Guyraud, P.; Essyem, N.; Vedrine, J. C. *Catal. Lett.* **1999**, *56*, 35.
(25) Corma, A.; Martinez, M.; Martinez, C. *J. Catal.* **1996**, *164*, 422.
(26) (a)Na, K.; Okuhara, T.; Misono, M. *J. Chem. Soc., Faraday Trans. 1* **1995**, *91*, 367. (b) Na. K.; Iizaki, T.; Okuhara, T.; Misono, M. *J. Mol. Catal.* **1997**, *115*, 449.
(27) Essayem, N.; Coudurier, G.; Fournier, M.; Vedrine, J. C. *Catal. Lett.* **1995**, *34*, 223.
(28) Kimura, M.; Nakato, T.; Okuhara, T. *Appl. Catal.* **1997**, *165*, 227.
(29) Okuhara, T.; Kimura, M.; Nakato, T. *Chem. Lett.* **1997**, 839.
(30) Okuhara, T.; Nishimura, T.; Watanabe, H.; Na, K.; Misono, M. *Acid−Base Catalysis II*; Kodansha: Tokyo and Elsevier: Amsterdam, 1994; p 419.
(31) Lee, K. Y.; Arai, T.; Nakata, S.; Asaoka, S.; Okuhara, T.; Misono, M. *J. Am. Chem. Soc.* **1992**, *114*, 2836.

Table 1. Estimated Crystallite Size and Particle Size of Cs Salts of $H_3PW_{12}O_{40}$

sample	evac.[a]	n[b]	SA[c] ($m^2 \cdot g^{-1}$)	d[d] (Å)	D[e] (Å)	LC[f] (Å)	ρ[g] ($g \cdot cm^{-3}$)
$H_3PW_{12}O_{40}$	r.t.	6.0	5	2264	510	12.17	5.3
	573 K	0	6	1887	390	12.18	5.3
$CsH_2PW_{12}O_{40}$	r.t.	4.0	2	5172	90	12.14	5.8
					302	12.01	5.6
	573 K	0	1	10712			5.6
$Cs_2HPW_{12}O_{40}$	r.t.	1.8	1	9523	128	11.86	6.3
	573 K	0	1	9677	134	11.86	6.2
$Cs_{2.5}H_{0.5}PW_{12}O_{40}$	r.t.	1.2	135	69	113	11.87	6.4
	573 K	0	135	69	120	11.87	6.4
$Cs_3PW_{12}O_{40}$	r.t.	0.3	147	63	105	11.88	6.5
	573 K	0	156	59	102	11.88	6.5
$Cs_2HPW_{12}O_{40}$(Imp)	573 K	0	3	3226	105	11.90	6.2
$Cs_{2.5}H_{0.5}PW_{12}O_{40}$(Imp)	573 K	0	134	70	96	11.84	6.4

[a] Evacuation temperature. [b] n is of the number of water molecules (crystallization water or adsorbed water) per 1 Keggin unit. [c] Surface area. [d] Size of particles estimated from the surface area. [e] Size of crystallites estimated from the XRD line width. [f] Lattice constant. [g] Density calculated from the lattice constant and molecular weight.

centrifugation into the supernatant and precipitate. The precipitate was dissolved in NaOH aqueous solution for analysis by ICP. The N_2 adsorption−desorption isotherm was measured at 77 K by an N_2 adsorption system (Micromeritics ASAP-2000) after the sample (50−200 mg) was evacuated at 573 K for 2 h. The surface area and the pore size distribution curve were calculated by the BET and BJH method,[32] respectively, after the evacuation at 573 K. The images of scanning electron microscopy (SEM) were taken with an S-900 FE-SEM (Hitachi) without Au deposition. Heat of NH_3 sorption was measured by using a calorimeter (Tokyo Rikou Co., HAC-450G). The catalyst (about 0.5 g) was pretreated in a vacuum at 473 K for 2 h prior to the sorption of NH_3 (Sumitomo Fine Chemical (99.99%)) and the heat of sorption was measured at 423 K. The NH_3 gas was dosed progressively to the sample with a pulse size of 20 μmol.

Results

Surface Area and Particle Size. The surface area, particle size, and crystallite size of these heteropoly compounds are summarized in Table 1. The particle size (d in diameter/Å) was estimated from the surface area according to an equation, $d = 60\,000/(\rho \times SA)$, where ρ is the density ($g \cdot cm^{-3}$) of the sample and SA is the surface area ($m^2 \cdot g^{-1}$). The value of ρ was estimated from the lattice constant and molecular weight. The crystallite size (D in diameter) was calculated from the Scherrer equation, $D = 0.9\lambda/(\beta - \beta_0) \cos \theta$, where λ is the X-ray wavelength (CuKα) in angstroms (1.54 Å), θ the diffraction angle, β the line width (in radians), and β_0 the instrumental line width (in radians). The lattice constants in Table 1 were determined from the diffraction angle on the basis of a bcc structure. The particle size (d) or crystallite size (D) corresponds to the size of the primary particle.

The surface area monotonically decreased as the Cs content increased from $x = 0$ to $x = 2$. But when the Cs content (x) exceeded 2, the surface area sharply increased. Particle sizes (d) estimated from the surface area were about 2000 Å for $H_3PW_{12}O_{40}$ and 5000−10000 Å for Cs1 and Cs2, respectively. On the other hand, the particle sizes (d) of Cs2.5 and Cs3 were 60−70 Å. It is noted that the crystallite size (D) from an XRD line width of Cs2 was close to those of Cs2.5 and Cs3, although d of Cs2 (5000−10000 Å) was greatly different. Cs1 evacuated at room temperature exhibited two sets of similar XRD patterns, of which the D values were 90 and 302 Å, respectively. The surface areas, particle sizes (d), and crystallite sizes (D) of Csx(Imp) were similar to those of the corresponding Csx (Table 1).

Table 2. Elementary Analysis Data of Precipitate, Supernatant, and Solid Obtained by Evaporation

(A) titration method[a]

	suspension[b]			
	solid (separated)[c]	supernatant		solid (evaporated)[d]
x[e]	Cs/polyanion	Cs (%)[f]	W (%)[f]	Cs/polyanion
1	2.0	5	52	1.1
2	2.1	2	11	2.2
2.5	2.4	2	2	2.4
3	3.0	0	0	3.0

(B) impregnation method[g]

	suspension[b]			
	solid (separated)[c]	supernatant		solid (evaporated)[d]
x[h]	Cs/polyanion	Cs (%)[f]	W (%)[f]	Cs/polyanion
1	2.1	1	83	1.1
2	2.2	4	21	1.8
2.5	2.5	1	3	2.6

[a] The aqueous solution of Cs_2CO_3 was added to the aqueous solution of $H_3PW_{12}O_{40}$ at room temperature. [b] Solid and supernatant in suspension were separated by centrifugation (see Experimental Section). The precipitates were separated by using centrifugation. [c] The values of Cs/polyanion correspond to 12 × Cs/W atomic ratios. [d] The suspension was directly dried to a solid by evaporation. [e] The ratio (in mol) of Cs added as Cs_2CO_3 to $H_3PW_{12}O_{40}$ used. [f] 100 × [the amount of Cs or W detected]/[the total amount of Cs or W used]. [g] The powder of Cs3 was dispersed into the aqueous solution of $H_3PW_{12}O_{40}$. [h] The ratio (in mol) of Cs in Cs3 to $H_3PW_{12}O_{40}$ added.

Elementary Analysis of the Suspension Containing Precipitates. The preparation process comprises precipitation, aging, drying by evaporation, and thermal treatment. Table 2 provides the results of elementary analysis of the solid and supernatant of the suspension formed by titration. The solid obtained by the evaporation of the suspension is shown as "solid (evaporated)" and the precipitate separated from the suspension by the centrifugation is expressed by "solid (separated)".

Cs1 (evaporated) and Cs2 (evaporated) gave the Cs/polyanion ratios of 1.1 and 2.2, respectively (the accuracy of the analysis is ±10%) (Table 2A). On the other hand, the Cs/polyanion ratios of Cs1 (separated) and Cs2 (separated) were close to 2. The quantity of Cs ion in the supernatant was always smaller than 5% that

(32) Barett, E. P.; Joyner, L. G.; Halenda, P. P. *J. Am. Chem. Soc.* **1951**, *13*, 373.

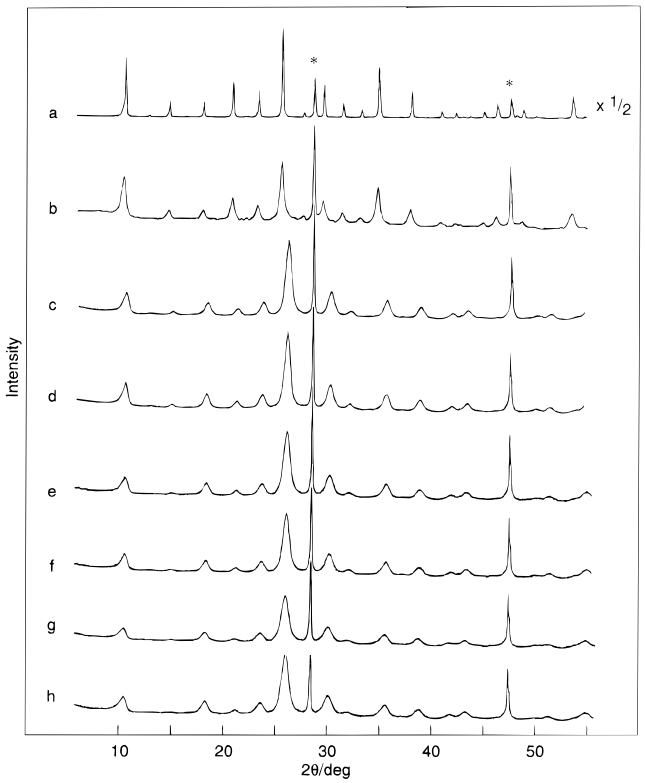

Figure 1. XRD patterns of $Cs_xH_{3-x}PW_{12}O_{40}$ prepared by the titration method. (a) $H_3PW_{12}O_{40}$ (r.t.), (b) $H_3PW_{12}O_{40}$ (573 K), (c) $Cs_2HPW_{12}O_{40}$ (r.t.), (d) $Cs_2HPW_{12}O_{40}$ (573 K), (e) $Cs_{2.5}H_{0.5}PW_{12}O_{40}$ (r.t.), (f) $Cs_{2.5}H_{0.5}PW_{12}O_{40}$ (573 K), (g) $Cs_3PW_{12}O_{40}$ (r.t.), and (h) $Cs_3HPW_{12}O_{40}$ (573 K). The evacuation temperature is shown in the parentheses. The peaks marked by * are due to Si used as the internal standard.

added. On the other hand, the amounts of polyanions (or W) remaining in the supernatant were 52% and 11%, that initially present for Cs1 and Cs2, respectively. For Cs2.5 and Cs3, the amounts of both Cs and W in the suspension were very small. Similar results were obtained in the impregnation method. Infrared spectra of Cs*x* and Cs*x*(Imp), which were taken by the KBr method, showed that the Keggin structure[9] remained intact.

X-ray Diffraction of $Cs_xH_{3-x}PW_{12}O_{40}$. Figure 1 provides XRD patterns of $H_3PW_{12}O_{40}$, Cs2, Cs2.5, and Cs3 after evacuation at room temperature or 573 K. $H_3PW_{12}O_{40}\cdot 6H_2O$ gave a pattern of the hexahydrate,[33] of which the lattice constant was 12.17 Å (Table 1). When the water of crystallization was removed, the XRD line widths increased (Figure 1b). The lattice constant of Cs2 evacuated at room temperature was 11.86 Å (Table 1). The variation of the peak positions of Cs2 by thermal treatment was less than 0.1 in 2θ (less than 0.04 Å in lattice constant). Cs2.5 and Cs3 gave XRD patterns similar to Cs2 and the changes of the XRD pattern upon thermal treatment were small. Cs2(Imp) and Cs2.5(Imp) behaved in essentially the same way as Cs2 and Cs2.5.

In Figure 2, the XRD patterns for Cs1 and Cs1(Imp) are provided. Both samples gave two sets of cubic XRD patterns. After evacuation at room temperature (Figure 2a,d), most peaks of Cs1 and Cs1(Imp) split. The lattice constants of the two sets were 12.14 and 12.01 Å for Cs1 and 12.14 and 11.96 Å for Cs1(Imp). When they

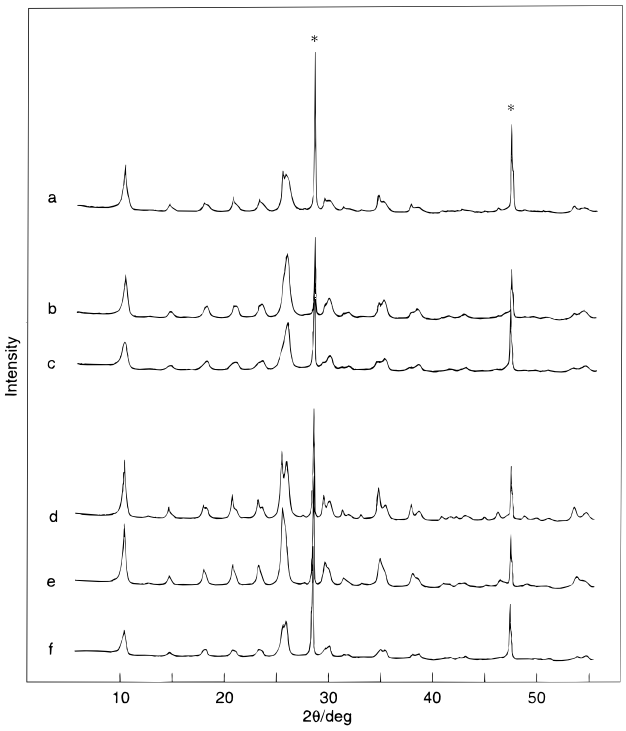

Figure 2. XRD patterns of $CsH_2PW_{12}O_{40}$. By the titration (a–c) and impregnation (d,e); evacuated at r.t. (a, d), 473 K (b, e), and 573 K (c, f). The peaks marked by * are due to Si.

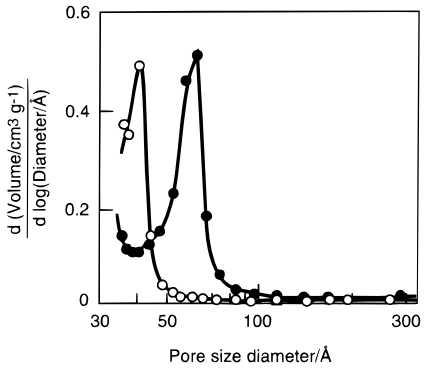

Figure 3. Pore size distribution curves by the BJH method. $Cs_{2.5}H_{0.5}PW_{12}O_{40}$ (○) and $Cs_3PW_{12}O_{40}$ (●). The experimental error is within 5% for this measurement.

were evacuated at 473 K, the two sets merged into one XRD pattern. The positions of new peaks were different from those before the evacuation.

Pore Size Distribution. $H_3PW_{12}O_{40}$, Cs1, and Cs2 exhibited Type II isotherms, which are ordinarily observed for nonporous materials.[34] A Type IV isotherm and a hysteresis loop in it were found for Cs2.5 and Cs3. The Type IV isotherm is usually observed for mesoporous materials.[34] Steep increases in the adsorption at low-pressure ranges ($p/p_0 < 0.1$) were observed, suggesting the presence of micropores for Cs2.5 and Cs3. Figure 3 shows mesopore-size distribution curves of Cs2.5 and Cs3 derived from the desorption branches by the BJH method.[32] The sharp peaks appeared at 40 and 60 Å in diameter for Cs2.5 and Cs3, respectively.

Scanning Electron Microscopy (SEM). Figure 4 provides the SEM micrographs of Cs2 and Cs2.5. The

(33) Brown, G. M.; Noe-Spirlet, M. R.; Busing, W. R.; Levy, H. A. *Acta Crystallogr.* **1977**, *B33*, 1038.

(34) Gregg, S. J.; Sing, K. S. W. *Adsorption, Surface Area and Porosity*; Academic Press: London, 1982.

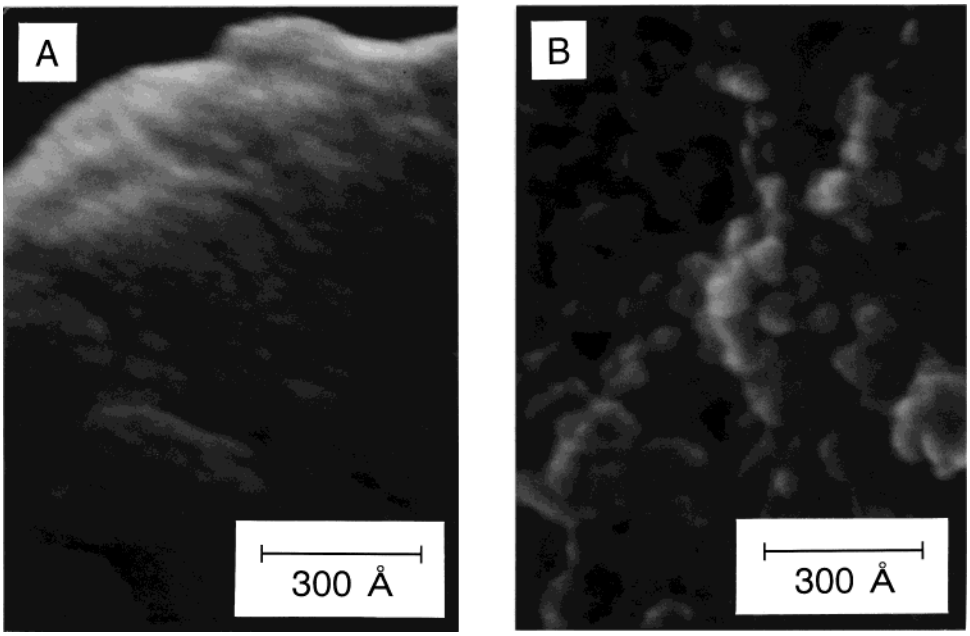

Figure 4. SEM images of $Cs_2HPW_{12}O_{40}$ (A) and $Cs_{2.5}H_{0.5}PW_{12}O_{40}$ (B).

surface of Cs2 is smooth (Figure 4A). Cs1 also showed a smooth surface (not shown). In contrast, Cs2.5 is composed of fine particles with the size of about 100 Å and the surfaces are rough (Figure 4B). As well as the primary spherical particles, pores between the particles can be seen for Cs2.5 (Figure 4B). Not shown, Cs3 gave a image similar to that of Cs2.5.

Solid-State NMR. As was reported previously,[35] $H_3PW_{12}O_{40}\cdot 6H_2O$ and anhydrous $H_3PW_{12}O_{40}$ gave peaks of ^{31}P at −15.6 and − 10.9 ppm, respectively. When the anhydrous $H_3PW_{12}O_{40}$ was exposed to air for a few minutes, the peak at −10.9 ppm shifted to −15.6 ppm. In Figure 5 are shown the ^{31}P NMR spectra of Cs1, Cs2, Cs2.5, and Cs3 pretreated at 473 K. Cs3 showed a single peak at −14.9 ppm (Figure 5d), which is close to that of $H_3PW_{12}O_{40}\cdot 6H_2O$. On the other hand, Cs1, Cs2, and Cs2.5 gave four peaks at −10.9, −12.2, −13.5, and −14.9 ppm and the relative intensities varied in a regular manner with the Cs content. The relative intensities of NMR peaks were in good agreement with the values calculated from the Cs/H ratio, r, by assuming binomial distributions, that is, $1{:}3r{:}3r^2{:}r^3$ for the peaks at −10.9, −12.1, −13.5, and −14.9.

Figure 6 shows the ^{31}P NMR spectra for Cs1(Imp), Cs2(Imp), and Cs2.5(Imp) after evacuation at 473 K (Cs*x*(Imp)'s are the acidic cesium salts prepared by impregnation of Cs3 with $H_3PW_{12}O_{40}$. See Experimental Section.). It is remarkable that these acidic salts, Cs*x*(Imp), showed four peaks at the same positions and almost the same relative intensities as those of Cs*x* (Figure 5).

Calorimetry of NH_3 Sorption. Figure 7 gives the results of calorimetry of NH_3 for $H_3PW_{12}O_{40}$ and Cs2.5 evacuated at 473 K. Initial heats of NH_3 sorption were about 195 and 170 kJ·mol^{-1} for $H_3PW_{12}O_{40}$ and Cs2.5, respectively. The amounts of NH_3 exhibiting the heat of sorption larger than 160 kJ·mol^{-1} were about 1.05 and 0.13 mmol·g^{-1} for $H_3PW_{12}O_{40}$ and Cs2.5, respectively. These values are very close to the number of protons in the whole bulk of $H_3PW_{12}O_{40}$ (1.04 mmol·g^{-1}) and Cs2.5 (0.155 mmol·g^{-1}).

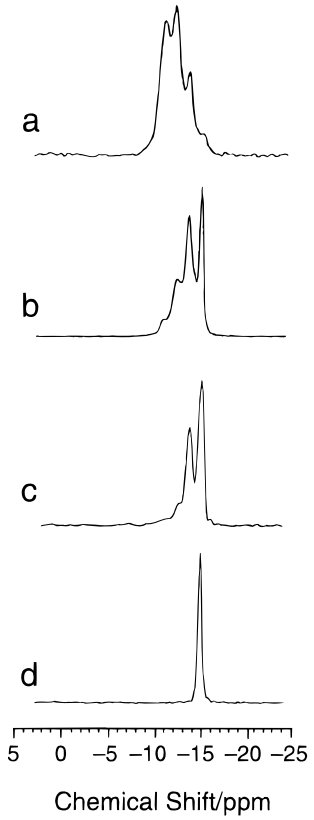

Figure 5. Solid-state ^{31}P NMR spectra of $Cs_xH_{3-x}PW_{12}O_{40}$ evacuated at 473 K. (a) $x = 1$, (b) $x = 2$, (c) $x = 2.5$, and (d) $x = 3$.

Discussion

To elucidate the unusual change in the surface area with the Cs content (Table 1),[17a] the formation processes and microstructure of the Cs salts must be clarified. This change is in a marked contrast with that of Na

(35) Kanda, Y.; Lee, K. Y.; Nakata, S.; Asaoka, S.; Misono, M. *Chem. Lett.* **1988**, 139.

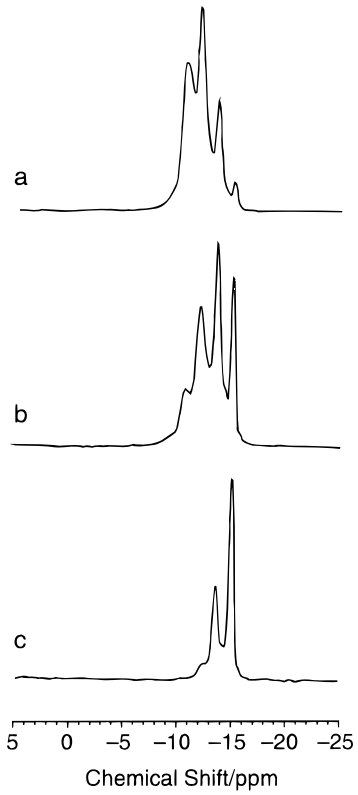

Figure 6. Solid-state ^{31}P NMR spectra of $Cs_xH_{3-x}PW_{12}O_{40}$(Imp). (a) $x = 1$, (b) $x = 2$, and (c) $x = 2.5$ evacuated at 473 K.

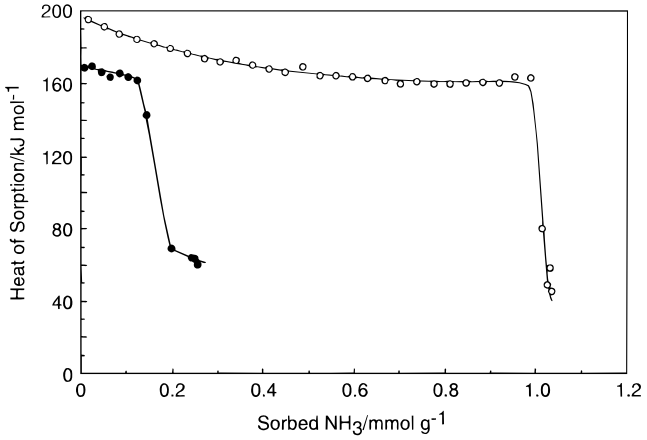

Figure 7. Differential heats of sorption of NH_3. (○) $H_3PW_{12}O_{40}$; (●) $Cs_{2.5}H_{0.5}PW_{12}O_{40}$. The catalysts were pre-evacuated at 473 K, and NH_3 was dosed at 423 K. The experimental error of this measurement is within 5%.

salts, of which the surface area monotonically decreased with the Na content.[17b] Contrary to the Na salts, Cs salts are insoluble and consist of fine crystallites, which are reasons for the unique surface area changes.[17a] Here, the compositions and formation processes of the Cs salts will be first described and then their microstructures. Last, the pore structure, surface acidity, and the catalysis will be discussed in relation to the microstructure.

Stoichiometry of the Precipitates. The supernatant at the preparation of Cs2.5 contained little Cs and W and the precipitates had the Cs/polyanion ratio of 2.4, which is close to the ratio of Cs added/polyanion = 2.5. Hence, eq 1 applicable for $2 \le x \le 3$ is deduced. For $x = 3$, the product is the stoichiometric salt, Cs3 = $Cs_3PW_{12}O_{40}$, and for the others ($2 \le x < 3$), $H_3PW_{12}O_{40}$ is probably epitaxially adsorbed on Cs3 and present in less than monolayer as discussed below.

From Cs2 to Cs3 ($2 \le x \le 3$),

$$PW_{12}O_{40}^{3-}(aq) + xCs^+(aq) + (3-x)H^+(aq) \rightarrow \text{“}Cs_xH_{3-x}PW_{12}O_{40}(s)\text{”} \quad (1)$$

It was remarkable that when the amount of Cs titrated was 1 or 2 in the ratio to polyanion (Table 2), the precipitates formed were expressed by “$Cs_2HPW_{12}O_{40}$”, as found in our early report.[19] After the titration, most of the Cs added was present in the precipitates for both cases. Hence, the formation of the precipitates for $1 \le x < 2$ must be described by eq 2. The amounts of W that remained in the supernatant (Table 2) were actually close to that expected from the second term of the right side of the equation.

From Cs1 to Cs2 ($1 \le x < 2$),

$$PW_{12}O_{40}^{3-}(aq) + xCs^+(aq) + (3-x)H^+(aq) \rightarrow (x/2)\text{“}Cs_2HPW_{12}O_{40}(s)\text{”} + (1-x/2)PW_{12}O_{40}^{3-}(aq) + (3-3x/2)H^+(aq) \quad (2)$$

There are two possibilities for “$Cs_2HPW_{12}O_{40}$”; that is, (1) the precipitate has a uniform composition of $Cs_2HPW_{12}O_{40}$ and (2) the precipitate is a mixture of, e.g., $H_3PW_{12}O_{40}$ and $Cs_3PW_{12}O_{40}$ (1:2 on average). In the case of Cs2, the single set of XRD was observed for “$Cs_2HPW_{12}O_{40}$” (Figure 1c,d). The XRD patterns and lattice constants before and after evacuation at 573 K agreed with those of Cs3 (Figure 1 and Table 1), showing that the single-crystal phase present in “$Cs_2HPW_{12}O_{40}$” is the same as that in Cs3.

From the above facts, a model can be proposed: Cs3 crystallites are formed at first, and then $H_3PW_{12}O_{40}$ is adsorbed epitaxially on the surface of Cs3 during the titration and drying. This model for Cs2 is verified by the results of Cs2(Imp) (Table 2 and Figure 2). Cs3 was impregnated with the aqueous solution of $H_3PW_{12}O_{40}$ to form a solid having the composition of “$Cs_2HPW_{12}O_{40}$”, that is, Cs2(Imp) (Table 2). As a matter of fact, the solid thus obtained gave the same XRD pattern as Cs3.

Considering the crystallite size (D) of Cs3 estimated by XRD (about 100 Å (Table 1)), we propose a model for “$Cs_2HPW_{12}O_{40}$” as illustrated in Figure 8A. This model is consistent with the stoichiometry as follows. If one assumes, for example, cubic-shape crystallites (primary particles) of Cs3 consisting of 8 polyanions on a side, one Cs3 particle comprises 512 ($=8^3$) polyanions. This size is reasonably assumed because the crystallite size of Cs3 is about 100 Å (Table 1) and the lattice constans are about 12 Å (Table 1). The number of the polyanions present in the outermost layer is about half (this corresponds to 296 polyanions) of the whole bulk. If $H_3PW_{12}O_{40}$ is adsorbed epitaxially on the surface of this Cs3 (Figure 8A), the number of $H_3PW_{12}O_{40}$ molecules corresponds to one-third of the total polyanions (808 polyanions) and the average composition of this particle (Cs3: $H_3PW_{12}O_{40}$ = about 2:1) becomes very close to $Cs_2HPW_{12}O_{40}$. Probably due to the equilibrium of adsorption−desorption of $H_3PW_{12}O_{40}$, a part of $H_3PW_{12}O_{40}$ (11% as shown in Table 2) is present in the solution.

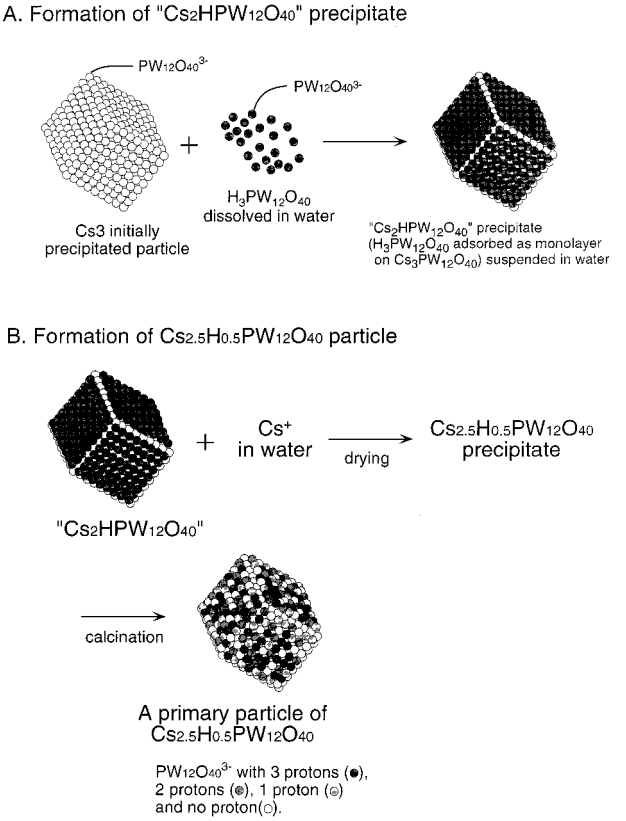

Figure 8. Proposed model for the formation of precipitate of $Cs_2HPW_{12}O_{40}$ (A) and the particle of $Cs_{2.5}H_{0.5}PW_{12}O_{40}$ (B).

In the case of the precipitate of Cs1 before thermal treatment, the observed two sets of XRD patterns are assignable to $H_3PW_{12}O_{40}\cdot 6H_2O$ and Cs3 (Figure 2). According to the results in Table 2, the suspension contains $H_3PW_{12}O_{40}$ in the supernatant, of which the amount is about half that added initially, and the suspended solid has the composition of "$Cs_2HPW_{12}O_{40}$" at the end of the Cs titration (Cs/polyanion = 1). After evaporation to dryness, most of the $H_3PW_{12}O_{40}$ is crystallized separately and the rest adsorbed on Cs3, forming a physical mixture of two kinds of particles, that is, $H_3PW_{12}O_{40}$ and "$Cs_2HPW_{12}O_{40}$" (1:1 in molar ratio). The stoichiometry observed is consistent with this model.

Structural Changes of Precipitates by Thermal Treatment. XRD and NMR data provide interesting information on the structural changes brought about by thermal treatments. The remarkable change in the XRD observed for Cs1 is that, after the thermal treatment at 473−573 K (Figure 2b and c), the two sets of XRD pattern became a single set, which is similar but distinctly different from the initial phases, i.e., $H_3PW_{12}O_{40}$ and Cs3. This fact indicates that the transformation from a mixture to a uniform solid solution took place.

The above transformation was confirmed by NMR measurements. To interpret the NMR spectra, the effects of desorption of water must be considered first. Dehydration of $H_3PW_{12}O_{40}\cdot 6H_2O$ caused the change in the peak position from −15.1 to −10.9 ppm in ^{31}P NMR, which is explained by the difference in the location of the acidic protons.[35] In $H_3PW_{12}O_{40}\cdot 6H_2O$, the acidic protons are all hydrogen-bonded to water of crystallization ($H_5O_2^+$) and no proton directly bonded to the bridging oxygen of the polyanion.[33] We presumed that, by the dehydration, three acidic protons move on to the bridging oxygen ($W-OH^+-W$).[36] The location of the proton is still controversial,[37] but our presumption is reasonable for the following reasons: (1) The bridging oxygen is shown to be most basic.[38] (2) Direct protonation at the bridging oxygen must have a stronger influence on the ^{31}P chemical shift than $H_5O_2^+$ hydrogen bonded to terminal oxygen. This is supported by the fact that the chemical shift of Cs3, which has no proton, was very close to that of $H_3PW_{12}O_{40}\cdot 6H_2O$. (3) The relative peak intensities of ^{31}P NMR for Cs*x* are very well interpreted on the basis of this idea as discussed below.

The peaks at the highest field (−14.9 ppm) and at the lowest field (−10.3 ppm) were detected for $H_3PW_{12}O_{40}\cdot 6H_2O$ and anhydrous $H_3PW_{12}O_{40}$, respectively. The former is assigned to the polyanion in which hydrated protons are hydrogen bonded to terminal oxygen according to the known crystal structure[33] and the latter to the polyanion having 3 protons directly bonded to the polyanion (most probably) at the position of the bridging oxygen.[33] As it is likely that the chemical shift changes with the number of protons attached, the two peaks (−12.9 and −13.1 ppm) located between the above two peaks can be assigned to the heteropolyanions having 1 and 2 protons at the bridging oxygen, respectively,[1,2,30] since each peak corresponds to the polyanion having a different number of protons (0, 1, 2, and 3).

The relative intensities of the ^{31}P NMR peaks were nearly equal to the binomial distributions, indicating that protons in these salts at least after evacuation above 473 K are distributed nearly uniformly through the whole bulk. The transformation of the two sets of the XRD pattern to a single set by the thermal treatment of Cs1 at 473 K (Figure 2) confirms that the migration of H^+ and Cs^+ actually occurred. The agreement of the NMR spectra between Cs*x*(Imp) and Cs*x* (Figures 5 and 6) further demonstrates that the protons mostly present on the surface at first result in a uniform distribution at least for $x \leq 1$. Essayem et al.[27] claimed from solid-state ^{31}P NMR measurement that when Cs2.5 is prepared from CsCl and washed, it consists of Cs3 and $H_3PW_{12}O_{40}$, even after thermal treatment. The difference in the preparation method must be responsible for the disagreement between the two studies.

Microstructure of Acidic Cs Salts after Thermal Treatment. As summarized in Table 1, the *D* values of Cs2.5 and Cs3 were 102−120 Å and *d* 59−69 Å. That is, *D* is comparable in order with *d*. This means that the powders of Cs2.5 and Cs3 consist of fine crystallites loosely aggregated. The differences between *D* and *d* are mostly due to the distribution of the crystallite size in these cases; the XRD line width reflects more the larger crystallites.

On the other hand, in the case of Cs2, *d* (about 10 000 Å) is very much larger than *D* (about 130 Å). Therefore, the particles of Cs2 must be nonporous dense aggregates of fine crystallites (polycrystallites). By the reason given below, the interstices between these primary particles

(36) Lee, K. Y.; Mizuno, N.; Okuhara, T.; Misono, M. *Bull. Chem. Soc. Jpn.* **1989**, *62*, 1731.
(37) Kozhevnikov, I. V.; Sinnenma, A.; Jansen, R. J. J.; Bekkum, H. *Catal. Lett.* **1994**, *27*, 187.
(38) Filowitz, M.; Ho, R. K. C.; Klemperer, W. G.; Shum, W. *Inorg. Chem.* **1979**, *18*, 93.

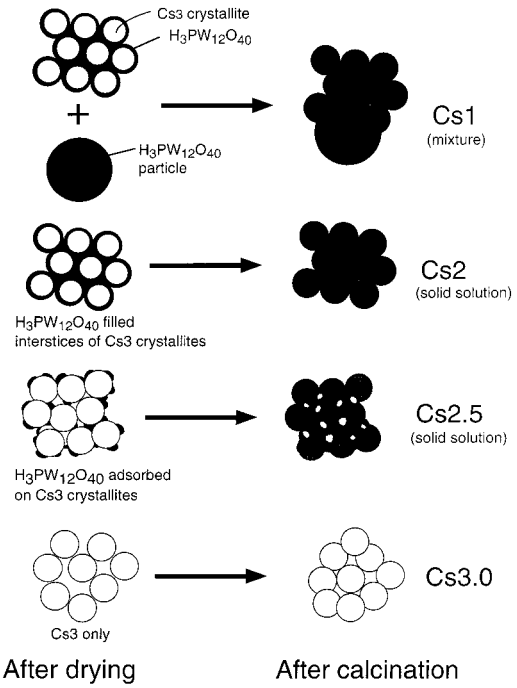

Figure 9. Proposed model for the formation of pores of $Cs_xH_{3-x}PW_{12}O_{40}$.

are filled by $H_3PW_{12}O_{40}$, which is adsorbed during titration and/or deposited during the drying. According to XRD, Cs1 was a mixture of crystallites having two different sizes (90 and 300 Å) (Table 1). The size, 300 Å, is close to that of $H_3PW_{12}O_{40}$ ($n = 0$ and 6), and the size, 90 Å, is comparable with those of Cs2.5 and Cs3. Therefore, Cs1 is most likely a mixture of $H_3PW_{12}O_{40}$ and Cs3 at first and becomes a solid solution after the thermal treatment.

SEM observations (Figure 4) clearly verify the microstructures of these salts as inferred above. The surface state and microstructure of Cs2.5 (and Cs3) were in a striking contrast with those of Cs2. Proposed models for the microstructure of $H_3PW_{12}O_{40}$ and Cs1−Cs3 are illustrated in Figure 9. It may be reminded that spherical secondary particles of Cs3 with the size of a few microns were formed by aging the solution at elevated temperatures.[39−41]

The isotherms of N_2 showed that $H_3PW_{12}O_{40}$, Cs1, and Cs2 are nonporous.[17a] On the other hand, Cs2.5 has both micropores and mesopores.[17a] The presence of the micropores was confirmed by Ar adsorption for Cs and NH_4 salts.[39] The hysteresis observed in the isotherm of Cs2.5 is due to the vaporization of nitrogen condensed in the mesopores. The desorption branch of the isotherm gives information on the neck of the pore.[34] The peak at 40 Å (Figure 3) for Cs2.5 shows that the mesopores possess neck and void structure, the size of the neck being about 40 Å in width. The desorption peak of Cs3 suggests the neck having the size of 60 Å.

The internal surface area of the mesopores was estimated from the pore size distribution in Figure 3 (35−100 Å) to be about 40 $m^2 \cdot g^{-1}$. This value corresponds to about 30% of the total surface area. The pores of Cs2.5 thus spread from mesopore to micropore and the latter contributes mainly to the surface area (70%). As we previously reported,[17a] 1,3,5-triisopropylbenzene (critical size, 8.5 Å) was adsorbed in most of the pores of Cs2.5. Therefore, the micropores of Cs2.5 are larger than 8.5 Å.

Next, the mechanism for the formation of pores of Cs2.5 and Cs3 is discussed. Moffat et al.[42] reported the presence of micropores for NH_4 and Cs salts and inferred that the pores are present in the crystal structure of the salts. On the other hand, Mizuno and Misono[43] reported that Cs3 had pores of about 80 Å, and the pores corresponded to voids between the primary particles (microcrystallites). If the size of the primary particles of Cs2.5 is about 100 Å, it is expected that the closest packed aggregates form the voids with the size of around 30 Å. The result of the present study is consistent with this mechanism. Therefore, the latter mechanism explains the mesopores of Cs2.5.

Proposed models for the tertiary structures and pores are provided in Figure 9. After the drying, small crystallites "$Cs_2HPW_{12}O_{40}$" aggregate to form large secondary particles. Amorphous small particles other than the crystallites likely fill in the interstices between the Cs3 core particles or precipitates in the interstices upon drying, resulting in the nonporous Cs1 and Cs2. In the case of Cs2.5, the amount of the amorphous heteropoly compound in the interstice is very small because the heteropolyacid is mostly consumed to form precipitates by the reaction with Cs^+. By this, the interstices between the particles are to a much lesser extent occupied. For Cs3, the voids themselves between the crystallite particles of Cs3 are pores since there is no more $H_3PW_{12}O_{40}$ remaining in the solution after titration.

As shown in Figure 7, the acid form gave the large value of heat of NH_3 sorption, which is consistent with the literature,[12] while this value includes Coulombic interactions in the solid lattice of ammonium salts because of the formation of ammonium salt. Cs2.5 showed also the high value, indicating that Cs2.5 has very strong acid sites.

Finally, the novel catalysis of Cs2.5 will be discussed. As reported previously,[13,17a,20−22] Cs2.5 exhibited high catalytic performance as solid acids particularly for reactions in the liquid phase. Cs2.5 was more active by about 2 orders of magnitude than $SiO_2-Al_2O_3$, sulfated ZrO_2, H-ZSM-5, and H_2SO_4 for decomposition of cyclohexylacetate and alkylation of 1,3,5-trimethylbenzene. One of the reasons for the higher activity of Cs2.5 is the strong acidity described above. In addition, the hydrophobic nature of the surface that was recently confirmed[44] may be an additional factor. The hydrocarbon reactants could be more efficiently activated on the surface of Cs2.5.

Among the acidic Cs salts ($Cs_xH_{3-x}PW_{12}O_{40}$), Cs2.5 was most active.[17a] This is due to the largest amount of

(39) (a) Yamada, T.; Johkan, K.; Okuhara, T. *Microporous Mesoporous Mater.* **1998**, *26*, 109. (b) Ito, T.; Inumaru, K.; Misono, M. *J. Phys. Chem. B* **1997**, *101*, 9958.
(40) Ito, T.; Song, I.; Inumaru, K.; Misono, M. *Chem. Lett.* **1997**, 727.
(41) Perez-Maqueda, L. A.; Matijivic, E. *Chem. Mater.* **1998**, *10*, 1430.
(42) McMonagle, J. B.; Moffat, J. B. *J. Colloid Interface Sci.* **1984**, *101*, 479. Moffat, J. B.; McMonagle, J. B.; Taylor, D. *Solid State Ionics* **1988**, *26*, 101.
(43) Mizuno, N.; Misono, M. *Chem. Lett.* **1987**, 967.
(44) Yamada, T.; Okuhara, T. *Langmuir* **2000**, *16*, 2321.

acid sites on the surface (surface acidity). The surface acidity was calculated from the surface area and the formal concentration of proton attached to polyanion, assuming that each polyanion on the surface possesses $(3-x)/2$ protons.[17a] The present study demonstrated that protons distribute almost uniformly through the whole bulk with the ^{31}P solid-state NMR and thus confirmed the above assumption. The mesoporous structure of Cs2.5 is another advantage for these reactions. Rapid diffusion of the reactants into the mesopores may be the reason for the high activities of these liquid−solid reactions, which is in contrast to the limitation of the diffusion into the micropores of H-ZSM-5.

Acknowledgment. This work was supported by the Grant-in-Aid for Scientific Research from the Ministry of Education, Science, Sports and Culture, Japan. The authors thank Prof. Shin-ichi Nakata (Akita University) for the measurements of solid-state NMR and heat of NH_3 sorption.

CM9907561